Pötz, S., Horsfield, B., Wilkes, H. (2014): Maturity-Driven Generation and Transformation of Acidic Compounds in the Organic-Rich Posidonia Shale as Revealed by Electrospray Ionization Fourier Transform Ion Cyclotron Resonance Mass Spectrometry. - Energy & Fuels, 28, 8, 4877-4888.

https://doi.org/10.1021/ef500688s

Maturity-driven Generation and Transformation of Acidic Compounds in the Organic-rich Posidonia Shale as revealed by Electrospray Ionization Fourier Transform Ion Cyclotron Resonance Mass Spectrometry

Stefanie Poetz[*]*, Brian Horsfield and Heinz Wilkes*

GFZ German Research Centre for Geosciences, Telegrafenberg, D-14473 Potsdam

KEYWORDS: Polar compounds, organic acids, carbazoles, maturity, shale oil, shale gas, Posidonia Shale, electrospray ionization, FT-ICR MS.

ABSTRACT

The Posidonia Shale in the Hils syncline in North-West Germany represents a natural maturity sequence from 0.48 to 1.45 % vitrinite reflectance (R_o). In this study, the molecular composition of the acidic compounds of six Posidonia Shale samples with a different maturation level has been determined using Fourier transform ion cyclotron resonance mass spectrometry (FT-ICR MS) combined with electrospray ionization (ESI) in the negative ion

mode. The changes in the distribution of elemental and compound classes as well as of double-bond equivalents (DBE) and carbon numbers at the different maturity levels are described in detail. Aromatic N_1, N_1O_1 and N_1S_1 compounds are preferably formed during ongoing maturation, while the amount of O_2 compounds decreases. With increasing thermal stress, condensation and aromatization of the acidic NSO compounds increases. In the sample of highest maturity (R_o 1.45%), which has been shown to have a relevant shale gas potential, a significant enrichment of non-alkylated and methylated highly aromatic N_1, N_1O_1 and N_1S_1 compounds has been observed, which can be the result of thermally induced side chain cracking of compounds with a higher alkylation degree. The other cracking products would be short chain hydrocarbons contributing to a significant amount to the overall gas potential of the Posidonia Shale.

1 Introduction

Shale gas refers to natural gas that was generated, and still confined, within fine grained dark grey - black sedimentary rocks such as mudstones and shales. This gas is disseminated within myriads of nm sized pores or adsorbed on mineral and organic particle surfaces within the rock, and can only be released by the controlled fracturing of the rock. Shale gas has been extensively exploited within the continental USA since the turn of the century from numerous plays, including the Barnett, Haynesville, Fayetteville, Marcellus, Antrim, Ohio and Woodford, and exploitation elsewhere has now begun, for example in the Peoples' Republic of China, Australia and Canada. The search has recently been extended to target "tight oil" reservoirs in shales of the U.S.A., Argentina and elsewhere, where thermal maturity levels are lower than those of shale gas plays. Shale gas and shale oil are of growing importance for the global energy supply. Worldwide, shale gas and oil make up a third of the technically recoverable total wet natural gas resources and 10% of the crude oil resources, respectively.[1] The development of resource plays in Europe is in its early infancy, with the Lower Carboniferous shales of northern England and the Lower Silurian shales of northern Poland being most advanced. Potentially prolific targets for shale gas production in Germany include the Lower Carboniferous, Lower Cretaceous and Lower Jurassic shales of northwest Germany. Here we use a natural laboratory of the Posidonia Shale in the Hils Syncline to investigate how changes in selected polar compound geochemistry are related to shale gas and shale oil potential.[2]

Besides maturity and type of the organic matter in the shale, the mineral rock properties like permeability, porosity or sorptive capacity have a large impact on the behavior of the organic compounds in the shale. On the other hand, the molecular structure of the organic compounds plays a major role. In contrast to the aliphatic and aromatic hydrocarbons, the organic compounds containing nitrogen, sulfur and oxygen (NSO compounds) possess functional

groups that cause an increased polarity which in turn may be modulated by shielding effects of alkyl substituents located at different positions within the molecules. Their structural diversity is the basis for a significant variability in physico-chemical properties resulting in different behavior during important physical and chemical processes in the shales.[3] The partition behavior of NSO compounds in such a multi-phase system with different solid (minerals, kerogen) and fluid (oil, water) phases is controlled by specific structure-property relationships governed by the presence or absence of certain functional groups, polarity, shielding effects and molecular size and shape. This in turn strongly influences expulsion efficiency and induces fractionation of different compound types. For example, the fractionation of certain carbazoles and benzocarbazoles in crude oils has been successfully correlated with migration distances in petroleum systems by Larter *et al.*.[3] However, there is clear evidence that in the Posidonia Shale thermal maturity influences the distribution of polar compounds like carbazoles to an at least equal extent.[4-6] Wilkes *et al.* described maturity related changes in the composition of various aromatic carbonyl compounds found in Posidonia shale samples like benzene-, naphthalene-, indane- and tetraline-based aldehydes and ketones.[7] As another example, carboxylic acids have also been applied successfully as indicators of maturation in petroleum systems.[8-9]

All of the studies mentioned above have in common that they were performed using gas chromatography coupled with mass spectrometry. As a consequence, the analytical window mainly covers low-polarity compounds within a mass range of *m/z* 50 – 300. Electrospray ionization combined with Fourier Transform ion cyclotron resonance mass spectrometry (ESI FT-ICR MS) enlarges the analytical window to compounds of low to high polarity within a mass range up to *m/z* 2000. ESI FT-ICR MS has been shown to be a highly suitable tool for the characterization of polar compounds in crude oils and bitumens.[10-17] ESI is a soft ionization method generating predominantly molecular ions. Operated in the negative ESI

mode, compounds containing an acidic hydrogen atom (mostly attached to a heteroatom) are selectively ionized by forming deprotonated species. Typically, carboxylic acids, phenolic compounds and carbazoles are main acidic constituents in petroleum fluids.[10-22] Besides whole oil samples, crude oil fractions gained by chromatographic or chemical sample pretreatment like low-, medium- or high-polarity compounds, acids, bases and asphaltenes were successfully characterized by this technique.[18-22] Among the unconventional fossil fuels, different shale oils obtained from immature oil shale samples from the USA, Russia and China have been characterized by ESI FT-ICR-MS.[23,24] The hydrotreatment of shale oils and the type of pyrolysis method applied for their generation had a significant influence on the molecular composition of the samples.[25-26]

The present paper provides a detailed insight into the acidic polar compound composition of six Posidonia Shale samples of different maturity. It describes and correlates the compositional changes with ongoing thermal maturation, proposes reaction pathways and derives new maturity parameters based on polar compounds. The contribution of polar compounds to gas generation within the Posidonia Shale is also considered.

2 Geological Setting/Study Area

The lower Toarcian Posidonia Shale is one of the most widespread and economically important oil source rocks of Western Europe. It was deposited during the Early Jurassic in an epicontinental sea of moderate depth stretching from the Yorkshire Basin over the Lower Saxony Basin to the Paris Basin. Only small connectivity existed among the Basins and between those and the open sea. Therefore, it can be assumed that deposition occurred in restricted environments with water stratification under prevailing anoxic conditions.

In the Hils Syncline, a topographic high about 100 km south of Hannover, northern Germany, the Posidonia Shale is approximately 35 m thick and subcrops at relatively shallow depth over

a 500 km^2 area. It displays a threefold stratigraphic subdivision: lower marlstone, middle calcareous shale with bivalve shells, and upper calcareous shale. The corresponding stratigraphic units are the Lias ε, Lias δ and Dogger formations. Sediments deposited in the Posidonia Shale contain Type II kerogen. Predominantly homogeneous depositional conditions and organic matter source have been revealed by detailed sedimentological and organic geochemical studies.[27-30,34] The Posidonia Shale of the Hils syncline has been well characterized and described in literature as a natural maturity sequence encompassing immature, mature and overmature zones with vitrinite reflectance (R_o) values increasing from 0.48 to 1.45 % from Southeast to Northwest. One possible explanation for the differences in maturity is the decreasing distance from an inferred deep-seated igneous intrusion, the Vlotho Massif, situated in the Northwest.[29] Six boreholes have been drilled completely penetrating the Posidonia Shale at different isoreflectance lines with R_o 0.48, 0.53, 0.68, 0.73, 0.88 and 1.48 %. At the highest studied maturity level (1.45 % R_o) the Posidonia Shale begins to fulfill the empirical organic geochemical criteria which designate it as a gas shale candidate.[32]

3 Experimental Section

3.1 Samples

We analyzed one core sample from the upper Lias ε formation of each of the 6 research boreholes in the Hils syncline. In the following, the six samples are named according to the name of the borehole location as WE (Wenzen), WI (Wickensen), DI (Dielmissen), DO (Dohnsen), HAR (Harderode) and HAD (Haddessen). Table 1 gives an overview of some general characteristics and selected bulk parameters for the sample set. The total organic carbon content (TOC) decreases from 12.2% at a vitrinite reflectance of R_o = 0.48 % to 6.9 % at R_o = 1.45 % and the extract yield expressed as the percentage of TOC decreases from 58.5 % to 17.7 %. The hydrogen index (HI) derived from Rock Eval pyrolysis decreases from 663

to 77 mg HC/g TOC. T_{max}, i.e. the temperature at which the maximum release of hydrocarbons from cracking of kerogen occurs during pyrolysis, shows an increase from 423 °C to 457 °C with increasing maturity. The relative amounts (related to the total amount of bitumen) of the acids, bases and high polar NSO compounds decrease while the amount of the medium polar NSO compounds remains constant for vitrinite reflectance values up to 0.88 % and then decreases. The low polar NSO compounds and the aromatic hydrocarbons show a fraction increase for R_o values of 0.48 to 0.73 % and a decrease at higher vitrinite reflectance values. In contrast, the amount of saturated hydrocarbons strongly increases with ongoing maturation.

3.2 Sample preparation

Core material was crushed and finely ground using a vibratory disc mill. A Soxhlet extractor was used for extraction of the Bitumen. 10 g of core sample material were filled in an extraction tube and extracted with a solvent mixture of dichloromethane and methanol (v:v = 99:1) at 40 °C for 24 hours. The extract yields were determined gravimetrically after removal of the solvent. A stock solution with a concentration of 1 mg/mL in methanol and toluene (v:v = 1:1) was prepared for each sample. Each stock solution was diluted with the same solvent mixture to give a final concentration of 100 µg/mL. 10 µL of a concentrated aqueous NH_3 solution were added to 1 mL sample solution to facilitate the deprotonation of the sample constituents.

3.3 FT-ICR MS analysis

Mass analyses were performed in negative ion ESI mode with a 12 Tesla FT-ICR mass spectrometer equipped with an Apollo II ESI source both from Bruker Daltonik GmbH (Bremen, Germany). Nitrogen was used as drying gas at a flow rate of 4.0 L/min and a temperature of 220 °C and as nebulizing gas with 1.4 bar. The sample solutions were infused at a flow rate of 150 µL/h. The capillary voltage was set to 3000 V and an additional CID

(collision-induced dissociation) voltage of 70 V in the source was applied to avoid cluster and adduct formation. Ions were accumulated in the collision cell for 0.05 s and transferred to the ICR cell within 1 ms. Spectra were recorded in broadband mode using 4 megaword data sets. For each mass spectrum, 200 scans have been accumulated in a mass range from *m/z* 147 to 1000. Sine-bell apodization was applied before the Fourier transformation was used to produce the frequency domain data, which was then converted to the mass spectrum.

3.4 Mass calibration and data analysis

An external calibration was done using an in-house calibration mixture for ESI negative mode containing fatty acids and modified polyethylene glycols.[33] Subsequently, each mass spectrum was internally recalibrated using known homologous series, e.g. the saturated fatty acids for the sample of lowest maturity and carbazoles with one, two and three additional fused aromatic rings for the shale samples with higher maturities. A quadratic calibration mode was chosen for all samples. The RMS errors of the six calibrations were between 0.001 and 0.031 ppm. Elemental formulas were assigned to the recalibrated *m/z* values with a maximal error of 0.5 ppm allowing 0 – 100 C, 0 – 200 H, 0 – 10 O, 0 – 4 N and 0 – 4 S atoms. Only single charged species were found in the spectra; therefore, *m/z* and mass are used synonymously in this paper. The number of assigned signals and the RMS errors of the exact masses of the assigned formulas of the four compound classes N_1, N_1O_1, N_1S_1 and O_2 are listed in Table 2. Data evaluation was done with the help of the software packages Data Analysis 4.0 SP5 (Bruker Daltonik GmbH, Germany), Composer 1.0.5 (Sierra Analytics Modesto, CA, USA) and Excel 2010 (Microsoft Corporation, Redmont, WA). Elemental formulas were sorted according to the sort of heteroatoms (elemental class), to their number of heteroatoms (compound class) and to the number of double bond equivalents (DBE) (DBE class). The DBE is a measure for the degree of unsaturation (or hydrogen deficiency) in a molecule and expresses the numbers of its double bonds (with at least one carbon atom) and rings. The DBE

is calculated for a molecule containing carbon, hydrogen, oxygen, sulfur, nitrogen and monovalent halogens $C_cH_hO_oN_nS_sX_x$ according to the formula DBE = c - 0.5* h +0.5 * n - 0.5 * x + 1. Please note that the numbers of oxygen and sulfur atoms are not included into the formula.

4 Results and Discussion

4.1 General chemical composition of the Posidonia Shale acids

ESI negative mass spectra

The ESI broadband mass spectra of the six Posidonia shale extracts are shown at the left side of Figure 1. The mass spectrum of the low maturity sample WE is dominated by peaks with odd nominal masses attributed to O_2 compounds by their exact mass. With increasing maturity, these compounds are depleted and peaks with even *m/*z values identified as N_1 compounds appear contemporaneously. The HAD sample shows the highest number of distinct N_1 peaks in its mass spectrum. As an additional feature, the spectra become more "thinned out" at higher maturities meaning that the number of distinct peaks increases while that of the peaks in the "hump" decreases. This is further illustrated for enlarged mass segments of two nominal masses in supplementary Figure SI 1. With increasing maturity the number of assigned monoisotopic peaks in each spectrum is reduced by half from more than 4600 to 2300 (Figure 1). The number average molecular weight (M_n) and weight average molecular weight (M_w) show no systematic variation with maturity (M_n: *m/z* 366.8 – 392.7, M_w: *m/z* 387.3 – 419.7, see Figure 1).

Elemental class distributions

The elemental class distributions of the Posidonia shale extracts are illustrated by pie charts shown at the right side of Figure 1. The O_x class dominates the immature sample WE. However, its fraction strongly decreases from 49.8 to 11.7 % of the total monoisotopic ion

abundance (TMIA) with increasing maturity. In contrast, the N_y fraction which is the most abundant elemental class in the sample HAD with highest maturity, is almost absent at the immature stage (1.9 % TMIA) and shows a strong increase up to 64.6 % TMIA with ongoing maturation. The N_yO_x class does not show a systematic trend but is fluctuating between 25 and 41 % in the samples with R_o values ≤ 0.88 % and is depleted to 14.6 % TMIA at R_o 1.45 %. The N_yS_z class rises from 0 % TMIA at a vitrinite reflectance of 0.48 % to 6.1 % TMIA at R_o 1.45 % while the O_xS_z class is depleted from 15.7 % TMIA to 1.1 % TMIA. The $O_xN_yS_z$ class is almost absent in sample WE and increases to 1.1% in sample HAD.

Compound class distributions

Figure 2 illustrates the maturation dependent changes of the compound class distributions in the four most abundant elemental classes. The N_y class consists mainly of N_1 compounds at all maturity levels. The relative abundance of the N_1 compound class increases from 2 % at low maturity to 62 % TMIA at highest maturity. The number of signals increases from 124 to 457 (Table 2). The N_2 compounds are present in much lower amounts but show a comparable increase from 0.05 % to 3 % TMIA. The dominance of the N_y compound class in the samples with higher maturity is consistent with negative ion ESI-FT-ICR-MS results for mature, not biodegraded crude oils reported by Hughey *et al.* and Shi *et al.*.[13, 18] In the N_yO_x class, the N_1O_1 compounds are most abundant (13 – 24 % TMIA) in all samples with R_o ≥ 0.68 %, while the N_1O_2 class is dominant (9 – 12 % TMIA) in samples with lower R_o values. The N_1O_3 class has the third highest abundance followed by N_2O_1 except for sample WI where N_2O_1 is more abundant than N_1O_3. In contrast to the N_1 class, the N_1O_1 class abundance increases from 4 – 24 % TMIA for vitrinite reflectance values up to 0.88 %, but then decreases to 10 % TMIA at 1.45 %. The signal number of N_1O_1 compounds shows the same trend (increase from 256 to 459 signals at 0.88 % followed by a decrease to 248 signals at 1.45 %, see Table 2). The N_yS_z class consists of almost only N_1S_1 compounds at all

maturities. The fraction of the N_1S_1 class increases from 0.2 to 5.5 % TMIA in the oil window and remains constant for the gas mature sample HAD. The signal number in the N_1S_1 class increases from 4 to 200 signals at R_o 0.88 % and decreases to 130 signals at R_o 1.45 % (Table 2). The O_2 class is the most abundant O_x class in all samples which comprises in addition the O_1 and the O_3 classes. In the immature WE sample, the O_2 class is the overall most abundant compound class. A similar dominance of the O_2 class was found in shale oils generated from Chinese and Russian oil shale.[23,24] The signal number of O_2 compounds decreases from more than 400 to 331 signals at highest maturity (Table 2). O_4 and O_5 compounds are found in the WE, WI, DO and DI samples and the WE sample also contains O_6 compounds.

4.2 Detailed characterization of selected compound classes

In the following sections, the N_1, N_1O_1, N_1S_1 and O_2 classes are described in more detail since they were found to experience major changes with increasing maturity. Each compound class is described with respect to its DBE class and its carbon number distribution.

N_1 compounds

The DBE class distribution of the N_1 class significantly changes with ongoing maturation (Figure 3a). The immature samples WE and WI have a monomodal distribution with DBE values of 9 – 20 and maximal relative intensities of 0.5 % and 1.8 % TMIA, respectively. In the samples of the lower oil window, DI and DO, all DBE classes increase, however, the DBE classes 12 and 15 are preferentially enriched, which most probably contain compounds consisting of a carbazole unit (a five-membered pyrrole ring fused with two benzene rings) and additional *ortho*-fused benzene rings like benzocarbazoles (12 DBE carbazoles) and dibenzo- or naphthocarbazoles (15 DBE carbazoles) (for compound structures, see Figure 3). Polycyclic ring systems in which any two adjacent rings have two, and only two, adjacent (carbon) atoms in common are called *ortho*-fused. 15 DBE carbazoles are most abundant in both samples. Sample HAR from the late oil window shows even higher intensities of 15

DBE and in addition 18 DBE carbazoles (benzonaphtho-, phenanthro- or anthracenocarbazoles). Here, 15 DBE carbazoles still are the most abundant species, but 18 DBE carbazoles are now more abundant than 12 DBE carbazoles. DBE classes containing *ortho*-fused carbazoles have been shown to make up a large fraction among the N_1 class in the resin and asphaltene fraction of a mature crude oil from the Liaohe oil field in Bohai Basin, China (DBE 9, 12, 15, 18), in a mature North American crude oil (DBE 9, 12) and in a Fushan shale oil, China (DBE 6, 9, 12).[13,18,25] Two additional DBE values, 20 and 23, become elevated in sample HAD, mainly representing the *ortho*- and *peri*-fused naphthopyreno- or benzobenzopyrenocarbazoles (20 DBE carbazoles) and phenanthrenopyreno-, anthracenopyreno-, naphthobenzopyreno- or benzodibenzo-pyrenocarbazoles (23 DBE carbazoles). A polycyclic ring system consisting of at least one ring *ortho*-fused to different sides of two other rings that are themselves *ortho*-fused together is said to be *ortho*-and *peri*-fused (examples of compound structures are found in Figure 3). *Ortho*- and *peri*-fused aromatic compounds have an increased aromaticity in terms of DBE density (DBE/C) compared to *peri*-fused ones. The DBE distribution of the sample from the gas window, HAD, indicates a decrease of N_1 compounds with a DBE value < 15 and a general increase of those with DBE values > 16. 18, 20 and 23 DBE carbazoles show a relatively stronger increase compared to other DBEs and 18 DBE carbazoles now make up the largest fraction. The intensity order of the carbazoles in this sample is 18 DBE > 15 DBE > 20 DBE > 23 DBE > 12 DBE.

Examplarily, the feature of carbon number distributions at the different maturity stages are described here in detail for the carbon number distributions of the 18 DBE N_1 compounds (see Figure 4 and Figure SI 2a in the supporting information). In all samples, compounds with carbon numbers of 24 – ~50 are detected showing an increase in peak intensity with increasing maturity within the oil window. However, for samples with R_o 0.88 and 1.45 %, N_1

compounds with 24 – 28 carbon atoms representing carbazoles with alkyl side chains of 0 – 4 carbon atoms (C_{0-4} 18 DBE carbazoles) are present to a much greater extent than the compounds with more than 28 carbon atoms representing in part the 18 DBE carbazoles with alkyl chains containing more than 4 carbon atoms ($C_{>4}$ 18 DBE carbazoles). These findings are consistent with published data on 12 and 15 DBE N_1 carbon number distributions in mature crude oils, shale oils and petroleum feedstock products.[13,18,25] The carbon number distribution in the HAD sample with the highest maturity reveals two major differences. First, the $C_{>4}$ carbazoles show a strong decrease compared to the samples with $R_o \leq 0.88\%$, and second, the sample shows a very steep rise in the amount of the 18 DBE compounds with 24 and 25 carbon atoms, which are the core and the mono methylated carbazole derivative, C_0 and C_1, respectively.

N_1O_1 compounds

For the N_1O_1 class the immature sample WE has a monomodal DBE distribution with DBE values in a range of 4 – 19 (Fig. 3b). WI shows an increased abundance of all DBEs and a slight preference of DBE 13. In the early oil window samples DI and DO, the DBE range shifts to higher values (8 – 25/26). Their DBE distributions have local maxima at DBE 10, 13, 15 and 18 (DI) and 10, 13, 15, 16, 18 and 21 (DO), respectively. Hydroxylated benzoquinolines ("benzoquinolinoles", e.g. acridinole) and the corresponding ketones containing a heteroaromatic 4-pyridinone ring unit ("benzoquinolinones", e.g. acridinone), both with 0 – 2 *ortho*-fused benzene rings, are part of DBE classes 10, 13 and 16 (molecular structures are shown in Figure 3). DBE 15, 18 and 21 very likely consist of molecules containing a pyrrolic ring and a cyclopenta-2,4-dien-1-one moiety as is found in fluorenone ("fluorenonocarbazoles") fused with 0 – 2 *ortho*-fused benzene rings (see Figure 3). Hughey *et al.* and Shi *et al.* also found elevated amounts of 15 and 18 DBE N_1O_1 compounds in a Smackover crude oil and in a Chinese shale oil, respectively.[13,18] Shi *et al.* suggested

hydroxylated carbazoles as possible core structures. They argued with the minimum carbon number found in the 15 and 18 DBE classes, which were 20 and 24, respectively. The minimum carbon numbers of the 12, 15 and 18 DBE N_1O_1 compounds in the Posidonia Shales are 15, 19 and 23 and therefore support the structure of fluorenonocarbazoles. At R_o 0.88 %, the amount of benzoquinolinoles/-ones remains constant while the fluorenonocarbazoles still increase. Within the fluorenonocarbazoles, the relative intensity order is DBE 18 > 15 > 21. Sample HAD has lost a great part of the acridinoles/-ones. The relative abundance of all DBE classes is relatively lower than in sample HAR. Interestingly, DBE classes 14, 17 and 20 containing compounds with pyrrolic nitrogen and a furan structure unit ("furanocarbazoles") are less abundant than the benzoquinolinoles/-ones at $R_o \leq 0.73$ % but become relatively enriched at higher maturities (structure shown in Figure 3).

The carbon number distribution of the 18 DBE class of fluorenonocarbazoles shown in Figure 4 (more detailed in Figure SI 2b) has in general similar features as those of the carbazoles. The immature samples show a monomodal broad distribution and with increasing maturity the oil and gas prone samples are dominated to increasing extents by N_1O_1 compounds with 23 to 27 carbon atoms representing the C_{0-4} 18 DBE fluorenonocarbazoles. In the HAD sample, the C_0 and C_1 compounds (N_1O_1 18 DBE compounds with 23 and 24 carbon atoms) make up a much larger fraction than in the samples of lower maturity. The carbon number ranges are extended in samples with vitrinite reflectance values of up to 0.88 % but are reduced at the highest maturity.

N_1S_1 compounds

The N_1S_1 DBE distributions of the early oil mature samples DI and DO have a range of 13 to 26 and local maxima at 14, 17 and 20 DBE with decreasing intensity in the order 17 > 14 > 20 (Fig. 3c). Compounds containing pyrrolic nitrogen and thiophenic sulfur ("thiophenocarbazoles", structures shown in Figure 3) are possible structures found in these

DBE classes. In HAR, the DBE range is expanded to 13 - 28 and the amounts of the 14, 17 and 20 DBE classes are increased. 17 DBE is still the most intense class, but the 20 DBE class now exceeds the 14 DBE class. In the gas window, the DBE range is now from 13 to 31, with an additional local maximum at 22 representing pyrenothiophenocarbazoles. The 14 and 17 DBE classes are depleted as all classes with DBE values <19. DBE classes with DBE values >19 are relatively enriched. A maturity-dependent relative enrichment of 14 and 17 DBE N_1S_1 compounds has also been observed in crude oils.[13]

The carbon number distributions of 17 DBE thiophenocarbazoles show comparable changes with increasing maturity as those found for the N_1 and N_1O_1 compounds (see Figure 4 and SI 2c). Starting with a monomodal distribution in the immature samples, the compounds with 22 to 26 carbon atoms ($C_{0\text{-}4}$ 17 DBE thiophenocarbazoles) are enriched in each DBE at higher maturities (see Figure 5c). In contrast to the carbazoles and most of the fluorenonocarbazoles (except N_1O_1 21 DBE), in the HAD sample, the C_2 compounds of the thiophenocarbazoles (e.g. N_1S_1 17 DBE with 24 carbon atoms) are more abundant than the C_0 and C_1 species. This may indicate that at this maturity stage the thermal energy is still too low to crack bonds between aromatic and aliphatic carbon atoms within a thiophenocarbazole molecule. Alternatively, it is possible that there is another family of N_1S_1 compounds with a different core structure consisting of 23 carbon atoms in the case of 17 DBE. For this core structure family, the compound with 23 carbon atoms would be C_0 and that with 24 carbon atoms C_1: the observed carbon number distribution would be a superposition of the carbon number distributions of the thiophenocarbazoles and the other core structure classes.

O_2 compounds

The DBE class distribution of the most abundant O_2 class shows a strong decrease of compounds with DBE values ≥ 5 (mainly aromatic carboxylic acids and diols) and a slight decrease of those with DBE values 2, 3 and 4 (naphthenic acids) at higher thermal maturities

(Figure 3d). The decrease does not occur continuously but stepwise with a higher gradient from 0.48 to 0.53 % and from 0.73 to 0.88 % vitrinite reflectance indicating greatest changes at the transition from the immature to oil window and from the oil to gas window. The amount of the fatty acids (DBE = 1), the dominant DBE class in all samples, decreases in the R_o range of 0.48 to 0.88 % and then increases in the overmature sample.

The changes in the carbon number distributions of DBE class 10 which consists mainly of aromatic carboxylic acids with increasing maturity is illustrated in Figure 4 and in the supporting information (Figure SI 2d). The aromatic acids in DBE class 10 have a carbon number range from 13 - ~43 for samples WE, WI, DI and DO and from 13 – 31 for samples HAR and HAD. The compounds with 18 to 45 carbon atoms are steadily lost with increasing maturity while those with 13 to 17 carbon atoms become enriched in the samples HAR and HAD. Possible chemical core structures with the elemental formula $C_{13}H_8O_2$ are hydroxyfluoren-9-one and acenaphthylenecarboxylic acid (structures are shown in Figure 3). The O_2 class with 6 DBEs is the most abundant DBE class in the immature samples WE and WI showing a carbon number range from 10 to 42 – 46 carbon atoms with a maximum at 20 carbon atoms (illustrated in Figure SI 3 in the supporting information). In addition, O_2 species with 6 DBE and carbon numbers between 28 and 36 likely representing hopanoic acids are relatively enriched in the most immature sample WE. The dominance of the C_{32} homologues is in agreement with the carbon number distributions of hopanoic acids found in modern sediments and other immature source rocks.[34-36] Their depletion with increasing maturity may be explained by decarboxylation reactions forming hopanes as proposed by Bennett and coworkers and Farrimond *et al.*.[36,37] The latter observed in immature source rocks hopane distributions maximizing at C_{31} comparing well with those of the hopanoic acids maximizing at one carbon number higher. The O_2 class with 5 DBEs (shown in the supporting information) has a carbon number range of 10 - ~40 in all samples. Compounds with 27, 28

and 29 carbon atoms representing among other compounds the steroidal acids cholestanic, ergostanic and stigmastanic acid are relatively enriched in the two immature samples but are depleted with ongoing thermal maturation. Like the hopanoic acids, the steroidal acids may be decarboxylated to steranes. Nevertheless, $C_{27\text{-}29}$ steranes and not $C_{26\text{-}28}$ steranes are predominantly found in source rocks at all maturities. However, if the carboxylic acid group in the observed steroidal acids is attached to one of the six-membered rings, the decarboxylation reaction would result in a molecule which is not recorded via the standard biomarker analysis (GC-MS fragment of *m/z* 203 instead of *m/z* 217).

4.3 Formation and transformation of N_1, N_1O_1 and N_1S_1 compounds

The results described in chapter 4.2 demonstrate that major compositional changes occur in the acidic compound fraction of the Posidonia Shale with ongoing maturation. Figure 4 summarizes these changes in the N_1, N_1O_1 and N_1S_1 classes for samples WE, DI, HAR and HAD in a color coded plot of DBE versus carbon number. The compositional variation is the result of at least one of the processes that take place during maturation, i.e. generation, transformation and expulsion of organic compounds. The generation of "new" compounds via thermal cracking reactions of the kerogen matrix appears to be the main process responsible for the increase of N_1, N_1O_1 and N_1S_1 compounds abundance at vitrinite reflectance values of 0.48 – 0.88 % (Scheme 1a), which is consistent with a generally high transformation ratio (54 %) of the initial kerogen into bitumen within this R_o range in the Posidonia Shales shown by Rullkötter and coauthors.[38] At higher maturities, only marginally more kerogen is transformed (56 % at R_o 1.45 %) as illustrated by the minor increase of N_1 compounds from the HAR to HAD sample. Besides, the average expulsion efficiency of oil and gas increases from 65 % at R_o = 0.68 % to 85 % (R_o = 0.88 %) to 96 % at R_o = 1.45 %.[38] Due to their molecular structure (involving functional groups), in particular the polar compounds are strongly controlled by the physical processes influencing the migration of petroleum out of the source rock. The main

processes are the adsorption on the surface of clay minerals and solid-liquid partitioning involving the different phases in a petroleum system, i.e. kerogen, minerals, bitumen, migrating petroleum and water. The accumulation of the condensed aromatic compounds like carbazoles, fluorenonocarbazoles and thiophenocarbazoles can be explained in different ways. First, the condensed aromatic molecules are to a high amount retained in the shale, while the less aromatic compounds migrate out of the source rock into the carrier bed during expulsion. And second, the kerogen matrix contains a large number of these structural moieties which are released in increasing amounts at increased maturity levels. If the first explanation would be correct, a depletion of these condensed aromatic compounds should be observed in expelled crude oils, which is not the case according to the literature.[10-18]

With proceeding maturation, the aromatization and condensation of the compounds in the Posidonia Shale increases, which is illustrated in Figure 4 by a shift of the compounds' DBE range to higher values (indicated with an arrow). Carbazoles, fluorenonocarbazoles and thiophenocarbazoles with higher annelation grades are enriched and *ortho*- and *peri*-fused molecules become more prominent compared to *ortho*-fused compounds. Again, two different explanations are possible: On the one hand, these compounds with higher DBE values may be released from the kerogen at higher maturities only. Since the probability for the cracking of compounds from the kerogen depends to a major extent on the strength of the aliphatic chain bonding between the core structures and not on the core structure types itself, this is not very likely. On the other hand, the compounds with higher DBEs could be formed via thermally-induced cyclization and aromatization reactions from carbazoles with lower DBE and alkyl side chains with a "summed" chain lengths of at least 4 carbon atoms at adjacent ring carbon atoms (illustrated in Scheme 1b for a C_9 12 DBE carbazole). Two *ortho*-substituted alkyl chains of the shown C_9 12 DBE carbazole undergo a cyclization leading to the formation of a six-membered saturated ring which is subsequently or even concurrently dehydrogenated. The

newly formed compound, a C_5 15 DBE carbazole, is characterized by a DBE increase of three and by a lower number of carbon atoms in the alkyl side chains. This reaction pathway also explains the depletion in long-chain alkylated carbazoles ($C_{<4}$ carbazoles) and increase of short chain carbazoles (C_{0-4} carbazoles) at high maturities, which can easily be recognized in Figure 6 as an reduction of carbon number range of each DBE class and a shift to lower carbon numbers. Another possible explanation for the depletion in $C_{<4}$ carbazoles would be the increased expulsion of long side chain core molecules due to their less effective retention on clay minerals.

The enrichment of C_0 and C_1 carbazoles in the overmature HAD sample can be the result of thermally induced side chain cracking (Scheme 1c). These secondary cracking reactions would lead to the formation of short chain hydrocarbons, e.g. methane or ethane, and therefore contribute to the gas generation in the Posidonia Shale. As outlined in Scheme 2, the proposed cyclization and aromatization reactions will provide sufficient hydrogen to facilitate the formation of gas hydrocarbons.

Degradation of N_1O_1 compounds

The N_1O_1 class abundance strongly decreases from 24 to 10% TMIA from the oil to the gas maturity range which is to the contrary as for the N_1 class. The decrease occurs evenly in all DBE classes. There are two possible interpretations for this finding. First, great parts of the N_1O_1 compounds have migrated out of the shale. An important argument against this scenario is that from the physico-chemical point of view there is no reason that the N_1O_1 compounds migrate, but the N_1 compounds do not. And second, N_1O_1 compounds are subject to thermal reactions changing their compound class affiliation. Decarbonylation of the keto-group in the fluorenone and benzoquinolinone units could be one possible reaction in such a scenario. According to Szabo et *al*., the decarbonylation of fluorenone yields a mixture of products

dominated by biphenylene and biphenyl.[39] Transferring this to the 15 DBE fluorenonocarbazoles means that the main products would be "biphenylenocarbazoles" (N_1 14 DBE) and "biphenylocarbazoles" (N_1 13 DBE), as illustrated in Scheme 2. If these reactions occur, a change of the carbon number distribution of the 13 and 14 DBE classes of N_1 and a relative enrichment of the $C_{0\text{-}4}$ biphenylenocarbazoles (N_1 14 DBE with 18 – 22 carbon atoms) and biphenylocarbazoles (N_1 13 DBE with 18 – 22 carbon atoms) would be expected. Figure 5 illustrates the carbon number distributions of the N_1 13 and 14 DBE classes which both show a relative enrichment of $C_{0\text{-}4}$ compounds especially in the overmature HAD sample, indicating that decarbonylation of keto group-containing compounds is a reaction that occurs during maturation.

4.4 New maturity parameters

The maturity related changes observed in the composition of the acidic N_1, N_1O_1, N_1S_1 and O_2 compounds of the Posidonia Shales lead us to suggest new maturity parameters. In this chapter, we focus on parameters derived from the N_1 class compounds, while those derived from the N_1O_1, N_1S_1 and O_2 class are described in the supporting information.

An almost linear positive correlation is found between the relative intensities of the N_1 class (% TMIA) and the vitrinite reflectance values in the samples of the immature and oil maturity range ($R_o \leq 0.88$ %) (Figure 6a). At higher maturity ($R_o = 1.45$ %), the N_1 class shows a further but less steep increase of relative abundance. In the same Figure, the sum of relative abundances of the DBE classes containing the *ortho*-fused carbazoles (N_1 DBE 9, 12, 15, 18, 21, 24, 27, 30, 33) on the one hand and the *ortho*- and *peri*-fused carbazoles (N_1 DBE 17, 20, 23, 26, 29, 32, 35) on the other hand are plotted against the vitrinite reflectance. The fraction of *ortho*-fused carbazoles shows the same trend as the whole N_1 class, but the *ortho*- and *peri*-fused carbazoles follow a linear increase over the whole maturity range. Among the individual DBE classes of the *ortho*-fused carbazoles, only those with higher DBE values of

18 and 21 show an increase of relative intensity over the whole range of vitrinite reflectance (Figure 6b), while lower DBE classes 12 and 15 do for samples with $R_o \leq 0.88$ % only. The DBE classes with *ortho*- and *peri*-fused carbazoles show similar features. The relative abundances of the individual DBE classes containing *ortho*- and *peri*-fused carbazoles, DBE 17, 20 and 23 (Figure 6c), increase with ongoing maturation over the whole maturity range.

If the mathematical relationship between the relative abundance of a class and the vitrinite reflectance is known, it can be used as a maturity parameter which has been calibrated for the study area investigated. Due to the restricted number of samples in the high maturity range (R_o 0.9 – 1.5 %) the choice of the mathematical function used for a nonlinear regression bears a high uncertainty. Therefore, we selected those parameters with a likely linear correlation of their relative abundance and the vitrinite reflectance values. The relative intensities of the total of *ortho*- and *peri*-fused, 18 DBE and 20 DBE carbazoles seem to show a linear increase with R_o (Figure 6). Linear regression was done for each of these three parameters based on the available six datapoints. The corresponding equations are

$y = 18.51 * x - 8.56$ (total of *ortho*- and *peri*-fused carbazoles)

$y = 10.39 * x - 4.59$ (N_1 18 DBE)

$y = 7.54 * x - 3.73$ (N_1 20 DBE)

These equations are restricted to the Posidonia Shale and cannot be applied to other shale gas systems. Their uncertainty due to the restricted number of data points must not be underestimated.

Figure 7a displays the mean DBE values of the total N_1 class and of the *ortho*-fused and *ortho*- and *peri*-fused carbazoles plotted against R_o. These three mean DBEs show a nonlinear increase over the whole vitrinite reflectance value range. In addition, the ternary diagrams

using the relative amounts of the most abundant DBE classes of *ortho*-fused (Figure 7b) and *ortho*- and *peri*-fused (Figure 7c) carbazoles are a promising tool for maturation assessment. For Posidonia Shale samples with a maturity ≤ 0.88 %, the data points of the *ortho*-fused DBE carbazoles are located on a straight line in the ternary diagram, while the data point of the HAD sample is not due to a relatively stronger decrease of 12 DBE compounds. In the ternary diagram of the *ortho*- and *peri*-fused carbazoles, the samples with vitrinite reflectance values ≥ 0.53 % plot on a straight line.

5 Summary and Conclusions

The acidic constituents of Posidonia Shale samples from the Hils Sincline show a high compositional variability controlled by maturity changes. Within the shale oil window, compounds from the N_1, N_1O_1 and N_1S_1 classes are released from the kerogen. With increasing maturity, the DBE values of these classes expressing the aromaticity of their constituents increases. Especially compounds with aromatic condensed ring systems are enriched with ongoing maturation (carbazoles, fluorenonocarbazoles, thiophenocarbazoles). At highest maturities, *ortho*- and *peri*-fused aromatic compounds are preferentially formed. Within the shale gas window, cracking of alkyl side chains occurs, leading to the release of natural gas hydrocarbons. Therefore, the thermal transformation of polar compounds in shales at high maturity significantly contributes to the shale gas potential. In this paper, we provide new insights into the detailed composition of polar compounds in the shale oil in the Posidonia Shale. New maturity parameters were introduced using the relative abundances of selected carbazole-containing classes, mean DBE values and relative amounts of selected DBE classes. Furthermore, it has been shown that ternary diagrams of relative intensities of *ortho*-fused and *ortho*- and *peri*-fused carbazoles can be used for maturity assessment.

Figures

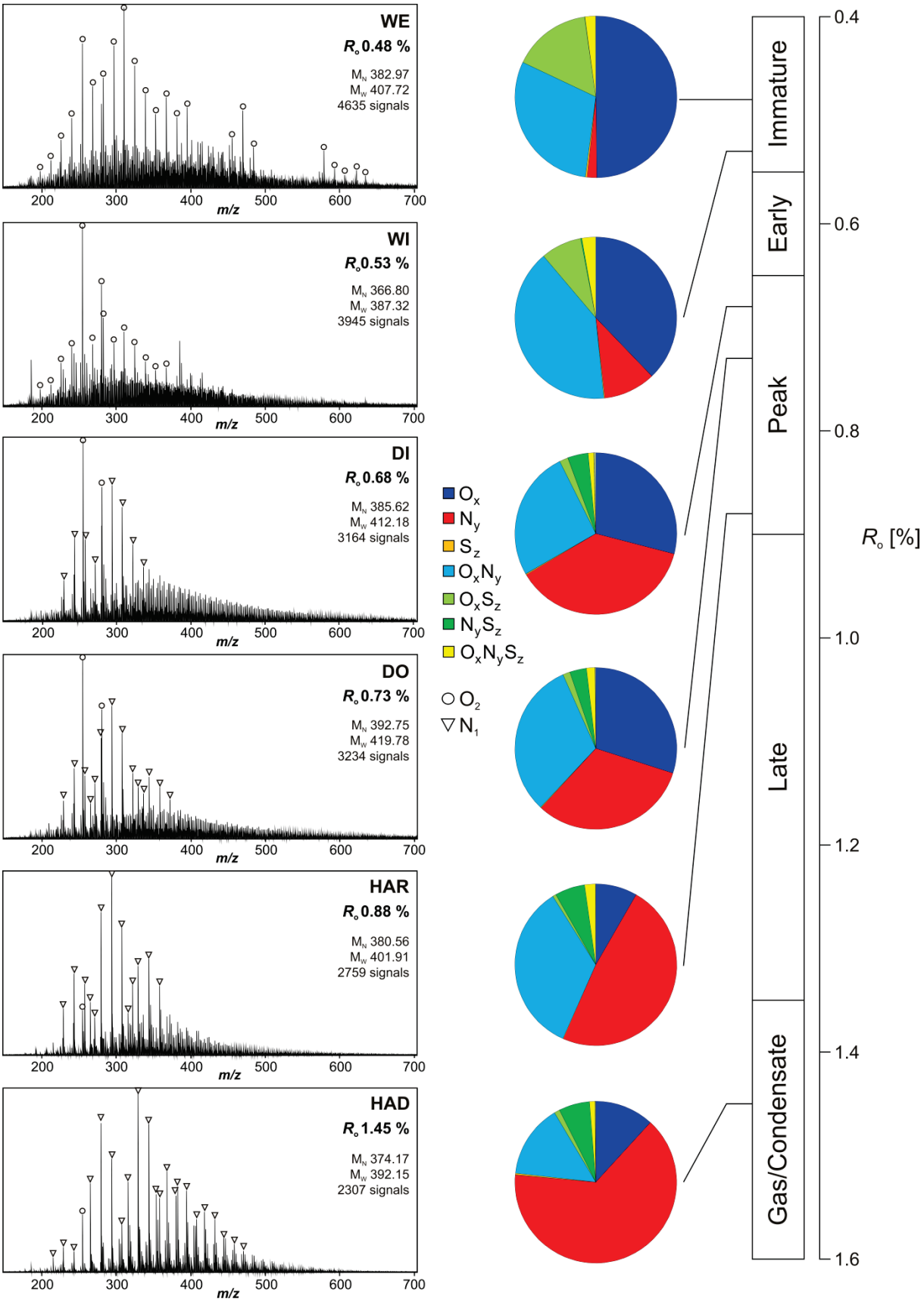
WE
R_o 0.48 %
M_N 382.97
M_W 407.72
4635 signals
WI
R_o 0.53 %
M_N 366.80
M_W 387.32
3945 signals
DI
R_o 0.68 %
M_N 385.62
M_W 412.18
3164 signals
DO
R_o 0.73 %
M_N 392.75
M_W 419.78
3234 signals
HAR
R_o 0.88 %
M_N 380.56
M_W 401.91
2759 signals
HAD
R_o 1.45 %
M_N 374.17
M_W 392.15
2307 signals
200 300 400 500 600 700
m/z
O_x
N_y
S_z
O_xN_y
O_xS_z
N_yS_z
$O_xN_yS_z$
O_2
N_1
Immature
Early
Peak
Late
Gas/Condensate
0.4
0.6
0.8
1.0
1.2
1.4
1.6
R_o [%]

Figure 1: Left: (-)-ESI Broadband spectra of the six Posidonia Shale samples with increasing maturity from top to bottom. Average molecular weights and number of signals are noted in the spectra. O_2 compounds are marked with open circles, N_1 compounds with open triangles. Right: Pie charts displaying the elemental class distribution of the peaks in the (-)-ESI spectra assigned with molecular formulas in the six Posidonia shale samples. Each pie chart is linked to a maturity window and the vitrinite reflectance value it belongs to (maturity scale after Peters and Moldowan 2005).[26]

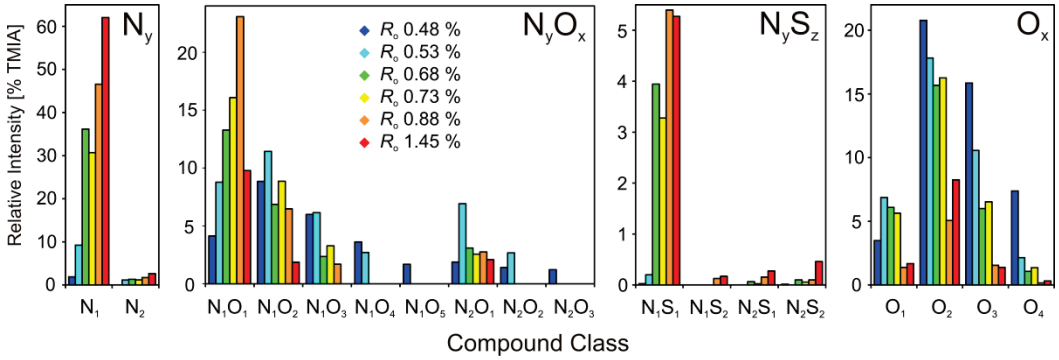

Figure 2: Compound class distribution of the N_y, N_yO_x, N_yS_z and O_x classes (from left to right) in the six Posidonia Shale samples.

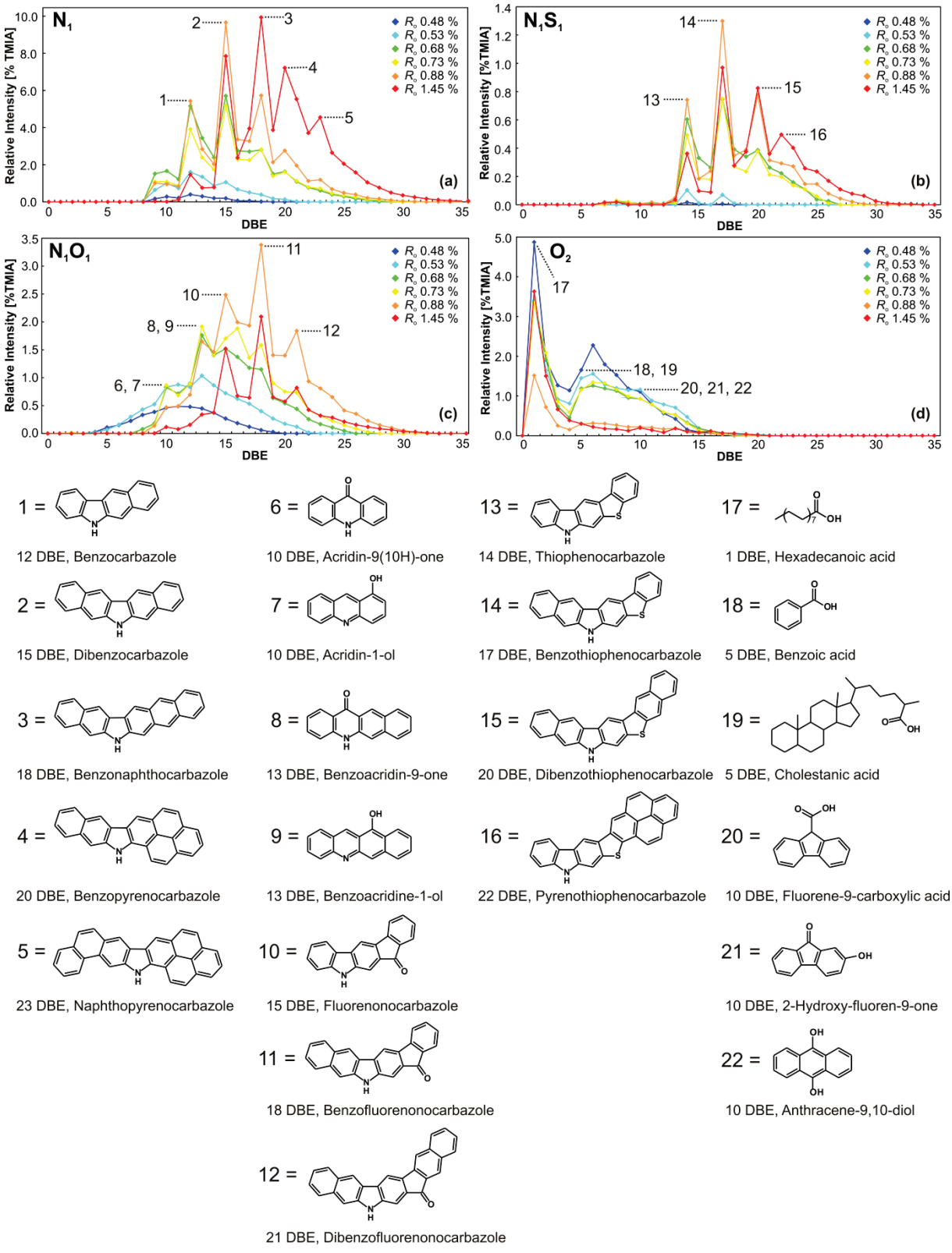

Figure 3: DBE distribution of the N_1 (a), N_1O_1 (b), N_1S_1 (c) and O_2 (d) classes in the six Posidonia Shale samples. For illustration, plausible core structures representing the respective DBE classes are also shown.

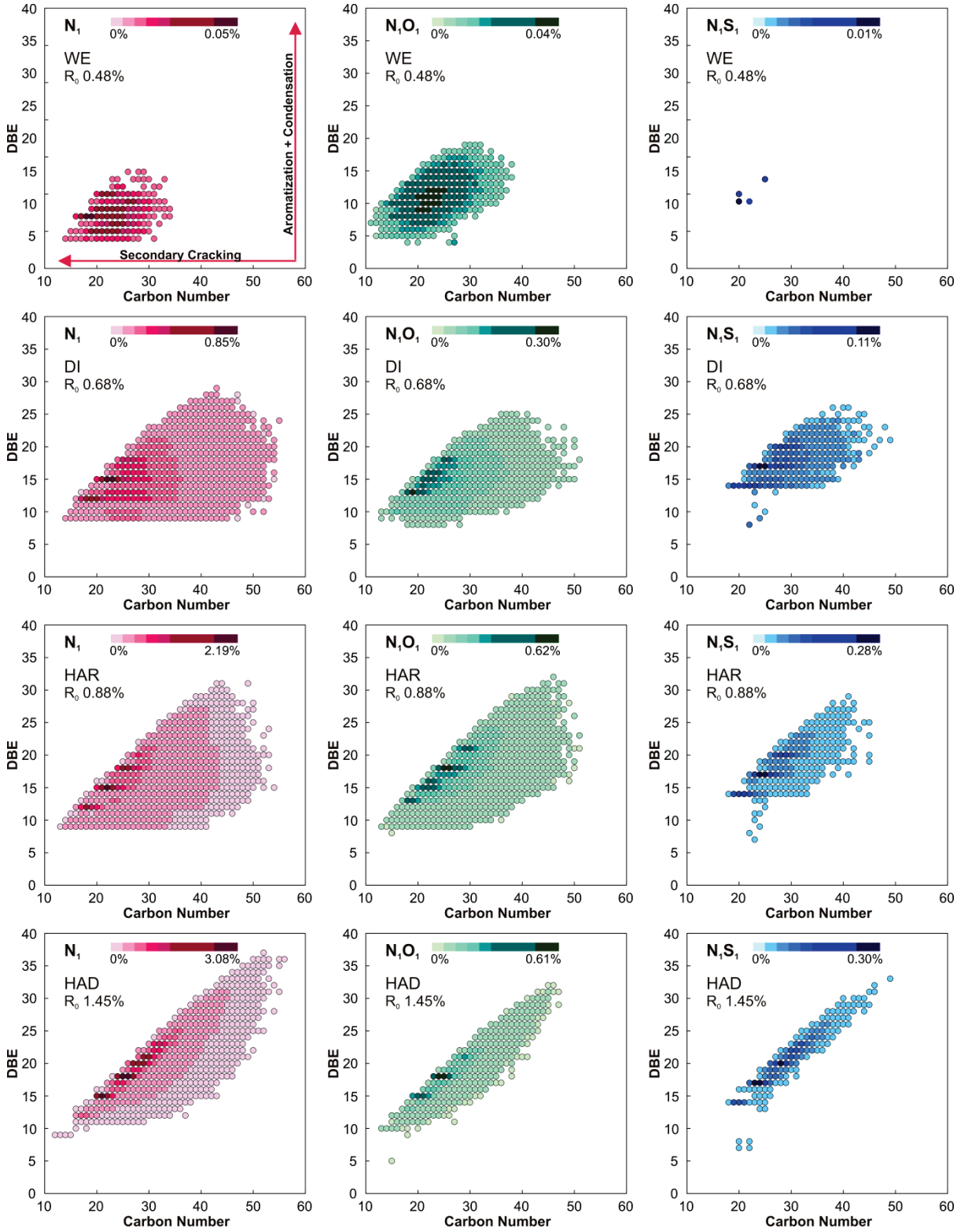

Figure 4: Color coded DBE versus carbon number plots of the N_1, N_1O_1 and N_1S_1 compounds for four selected Posidonia Shale samples (from top to bottom: WE, DI, HAR, HAD).

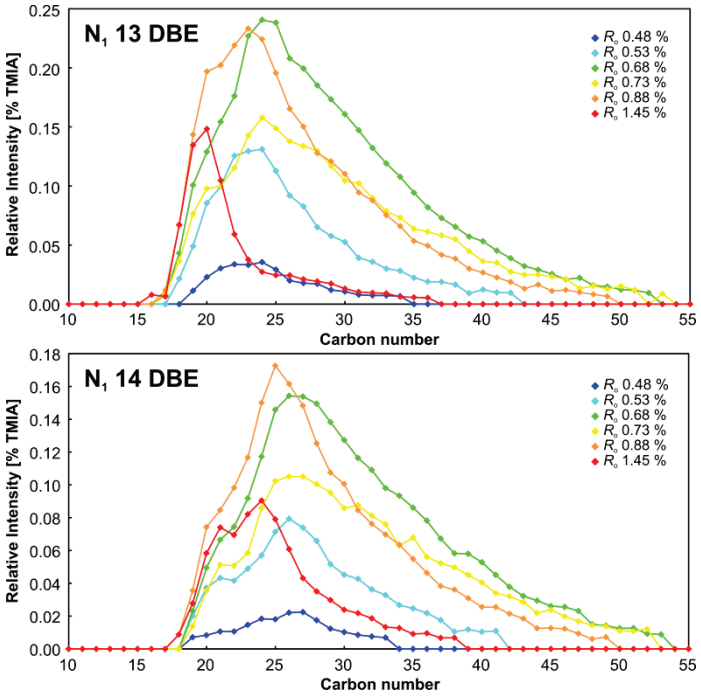

Figure 5: Carbon number distributions of N_1 13 DBE and N_1 14 DBE classes in the six Posidonia Shale samples.

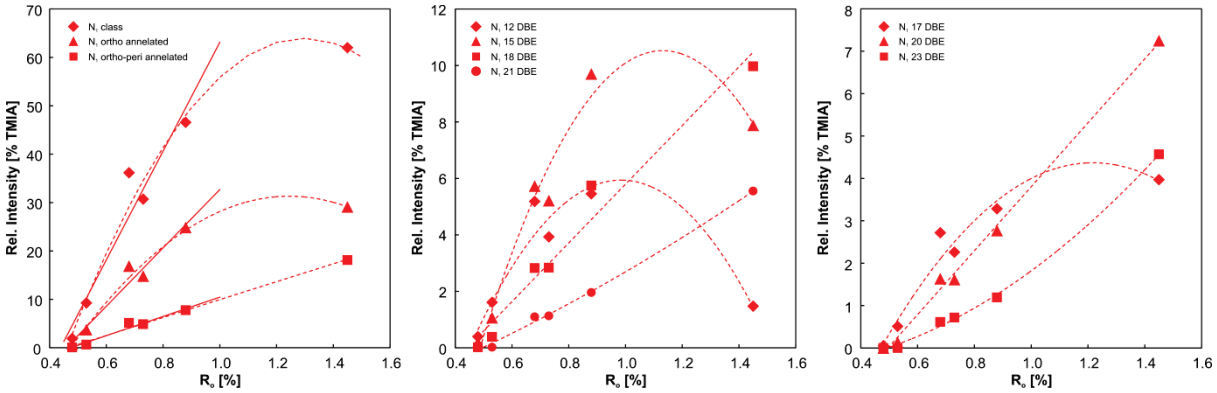

Figure 6: Maturity-related changes in relative abundances of a) the N_1 compound class, the *ortho*-fused and the *ortho*- and *peri*-fused carbazoles; b) the individual DBE classes of the *ortho*-fused carbazoles and c) the individual DBE classes of the *ortho*- and *peri*-fused carbazoles.

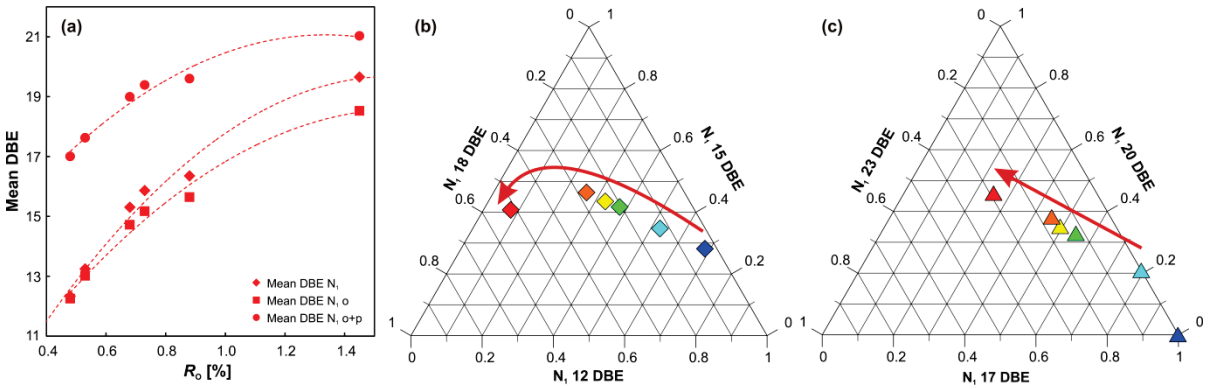

Figure 7: Maturity-related changes of the calculated mean DBEs of the N_1 compound class, *ortho*-fused carbazoles and *ortho*- and *peri*-fused carbazoles (a). Ternary diagram for the most abundant DBE classes of the *ortho*-fused carbazoles (b) and *ortho*- and *peri*-fused carbazoles (c).

Schemes

a) Release of N_1 compounds from the kerogen matrix via thermal cracking

b) Thermally-induced cyclization and aromatization

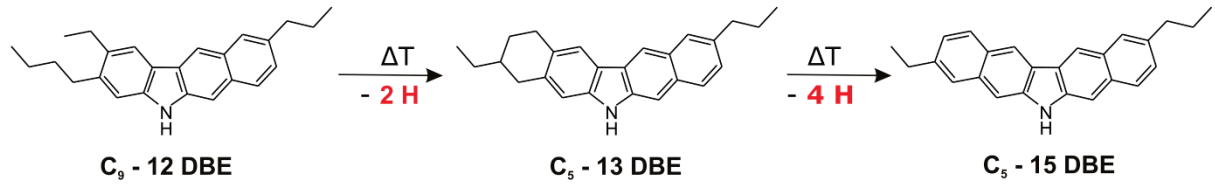

c) Thermally-induced cracking of side chains

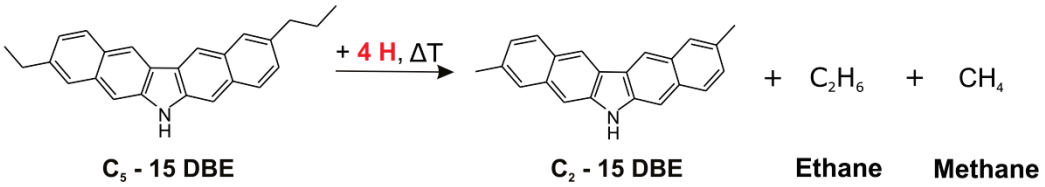

Scheme 1: Possible reaction pathways occurring during maturation.

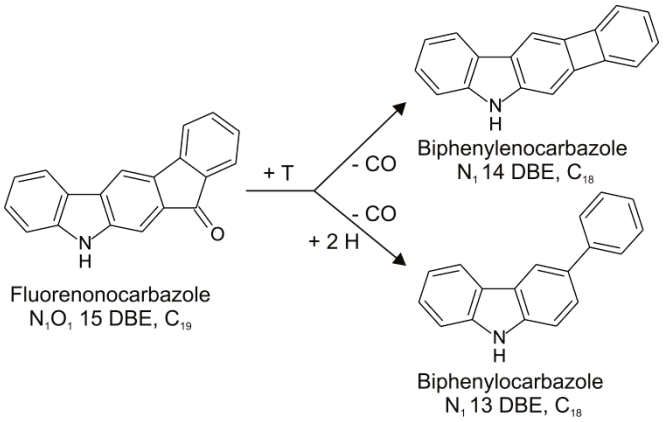

Scheme 2: Possible degradation pathways of N_1O_1 compounds (decarbonylation of fluorenonocarbazoles) occurring at high maturity (R_o > 0.88 %).

Tables

Table 1: Bulk parameters for geochemical characterization of organic matter in sediment samples from the six boreholes in the Hils syncline, northern Germany.

Borehole	**Wenzen**	**Wickensen**	**Dielmissen**	**Dohnsen**	**Harderode**	**Haddessen**
Abbreviation	WE	WI	DI	DO	HAR	HAD
R_o [%]	0.48	0.53	0.68	0.73	0.88	1.45
TOC [%]	12.2	13.4	8.1	9.4	6.3	6.9
HI [mg HC/g TOC]	663	617	574	429	363	77
T_{max} [°C]	423	427	438	445	444	457
Bitumen [% TOC]$_l$	58.5	61.8	72.6	67.2	92.0	17.7
Acids [% Bitumen]	9.7	5.0	1.4	1.2	1.4	0.6
Bases [% Bitumen]	3.1	2.3	1.5	0.9	1.3	0.6
High Polars [%Bitumen]	24.8	14.2	5.4	3.9	4.3	1.1
Medium Polars [%Bitumen]	10.4	9.9	9.8	3.7	8.7	2.8
Low Polars [%Bitumen]	18.3	19.7	27.4	23.2	21.7	9.6
Aromatics [%Bitumen]	10.1	7.8	20.9	16.8	17.3	12.4
Saturates [%Bitumen]	7.9	15.9	15.0	8.2	25.8	40.1

Data are average values for a different number of samples per borehole and taken from Wilkes *et al.*.[4] R_o: vitrinite reflectance, TOC: total organic carbon content, HI: hydrogen index, T_{max}: temperature at which the maximum release of hydrocarbons from cracking of kerogen occurs during pyrolysis.

Table 2:Number of signals, average molecular weights and root mean square (RMS) errors of all and selected (N_1, N_1O_1, N_1S_1 and O_2) compounds and their calculated molecular formulae.

	Number of Signals					**M_n**	**M_w**	**RMS Error [ppm]**			
Sample	**Total**	**N_1**	**N_1O_1**	**N_1S_1**	**O_2**	**Total**	**Total**	**N_1**	**N_1O_1**	**N_1S_1**	**O_2**
WE	4635	124	256	4	416	382	407	0.046	0.055	0.044	0.081
WI	3945	255	325	13	402	366	387	0.053	0.068	0.073	0.055
DI	3164	533	382	202	409	385	412	0.124	0.091	0.108	0.053
DO	3234	524	428	163	433	392	419	0.109	0.102	0.075	0.061
HAR	2759	525	459	200	279	380	401	0.096	0.097	0.103	0.038
HAD	2307	457	248	130	331	374	392	0.116	0.075	0.116	0.061

Number of signals: number of assigned, monoisotopic signals, M_n: number average molecular weight, M_w: weight average molecular weight, RMS: root mean square.

Literature

(1) Eia, U.S. Energy Information Administration Technically recoverable shale oil and shale gas ressources: an assessment of 137 shale formations in 41 countries outside the United States, Report June **2013**.

(2) Horsfield, B. Shale gas in the Posidonia Shale, Hils area, Germany. *Search and Discovery* **2010**, *#110126*.

(3) Larter, S. R.; Bowler, B. F. J.; Li, M.; Chen, M.; Brincat, D.; Bennett, B.; Noke, K.; Donohoe, P.; Simmons, D.; Kohnen, M.; Allan, J.; Telnaes, N.; Horstad, I. Molecular indicators of secondary oil migration distances. *Nature* **1996**, *383* (6601), 593-597.

(4) Horsfield, B.; Clegg, H.; Wilkes, H.; Santamaria-Orozco, D. Effect of maturity on carbazole distributions in petroleum systems: new insights from the Sonda de Campeche, Mexico, and Hils Syncline, Germany. *Naturwissenschaften* **1998**, *85* (5), 233-237.

(5) Clegg, H.; Wilkes, H.; Horsfield, B. Carbazole distributions in carbonate and clastic source rocks. *Geochim Cosmochim Ac* **1997**, *61* (24), 5335-5345.

(6) Wilkes, H.; Clegg, H.; Disko, U.; Willsch, H.; Horsfield, B. Fluoren-9-ones and carbazoles in the Posidonia Shale, Hils Syncline, northwest Germany. *Fuel* **1998**, *77* (7), 657-668.

(7) Wilkes, H.; Disko, U.; Horsfield, B. Aromatic aldehydes and ketones in the Posidonia shale, Hils syncline, Germany. *Org Geochem* **1998**, *29* (1-3), 107-117.

(8) Mackenzie, A. S.; Lamb, N. A.; Maxwell, J. R. Steroid hydrocarbons and the thermal history of sediments. *Nature* **1982**, *295* (5846), 223-226.

(9) Jaffé, R.; Gardinali, P.; Wolff, G. A. Evolution of alkanes and carboxylic acids in ancient sediments from the Maracaibo Basin. *Org Geochem* **1992**, *18* (2), 195-201.

(10) Qian, K. N.; Robbins, W. K.; Hughey, C. A.; Cooper, H. J.; Rodgers, R. P.; Marshall, A. G. Resolution and identification of elemental compositions for more than 3000 crude acids in

heavy petroleum by negative-ion microelectrospray high-field Fourier transform ion cyclotron resonance mass spectrometry. *Energy Fuel* **2001**, *15* (6), 1505-1511.

(11) Hughey, C. A.; Rodgers, R. P.; Marshall, A. G. Resolution of 11 000 compositionally distinct components in a single Electrospray ionization Fourier transform ion cyclotron resonance mass spectrum of crude oil. *Anal Chem* **2002,** *74* (16), 4145-4149.

(12) Pakarinen, J. M. H.; Teravainen, M. J.; Pirskanen, A.; Wickstrom, K.; Vainiotalo, P. A positive-ion electrospray ionization Fourier transform ion cyclotron resonance mass spectrometry study of Russian and north sea crude oils and their six distillation fractions. *Energy Fuel* **2007**, *21* (6), 3369-3374.

(13) Hughey, C. A.; Rodgers, R. P.; Marshall, A. G.; Walters, C. C.; Qian, K. N.; Mankiewicz, P. Acidic and neutral polar NSO compounds in Smackover oils of different thermal maturity revealed by electrospray high field Fourier transform ion cyclotron resonance mass spectrometry. *Org Geochem* **2004**, *35* (7), 863-880.

(14) Hur, M.; Yeo, I.; Kim, E.; No, M. H.; Koh, J.; Cho, Y. J.; Lee, J. W.; Kim, S. Correlation of FT-ICR Mass Spectra with the Chemical and Physical Properties of Associated Crude Oils. *Energy Fuel* **2010**, *24*, 5524-5532.

(15) Teravainen, M. J.; Pakarinen, J. M. H.; Wickstrom, K.; Vainiotalo, P. Comparison of the composition of Russian and North Sea crude oils and their eight distillation fractions studied by negative-ion electrospray ionization Fourier transform ion cyclotron resonance mass spectrometry: The effect of suppression. *Energy Fuel* **2007**, *21* (1), 266-273.

(16) Hughey, C. A.; Galasso, S. A.; Zumberge, J. E. Detailed compositional comparison of acidic NSO compounds in biodegraded reservoir and surface crude oils by negative ion electrospray Fourier transform ion cyclotron resonance mass spectrometry. *Fuel* **2007**, *86* (5-6), 758-768.

(17) Liao, Y.; Shi, Q.; Hsu, C. S.; Pan, Y.; Zhang, Y. Distribution of acids and nitrogen-containing compounds in biodegraded oils of the Liaohe Basin by negative ion ESI FT-ICR MS. *Org Geochem* **2012**, *47* (0), 51-65.

(18) Shi, Q. A.; Zhao, S. Q.; Xu, Z. M.; Chung, K. H.; Zhang, Y. H.; Xu, C. M. Distribution of acids and neutral nitrogen compounds in a Chinese crude oil and its fractions: characterized by negative-ion electrospray ionization Fourier transform ion cyclotron resonance mass spectrometry. *Energy Fuel* **2010**, *24*, 4005-4011.

(19) Gaspar, A.; Zellermann, E.; Lababidi, S.; Reece, J.; Schrader, W. Characterization of saturates, aromatics, resins, and asphaltenes heavy crude oil fractions by atmospheric pressure laser ionization Fourier transform ion cyclotron resonance mass spectrometry. *Energy Fuel* **2012**, *26* (6), 3481-3487.

(20) Cho, Y.; Kim, Y. H.; Kim, S. Planar limit-assisted structural interpretation of saturates/aromatics/resins/asphaltenes fractionated crude oil compounds observed by Fourier transform ion cyclotron resonance mass spectrometry. *Anal Chem* **2011**, *83* (15), 6068-6073.

(21) Klein, G. C.; Angstrom, A.; Rodgers, R. P.; Marshall, A. G. Use of saturates/aromatics/resins/asphaltenes (SARA) fractionation to determine matrix effects in crude oil analysis by electrospray ionization Fourier transform ion cyclotron resonance mass spectrometry. *Energy Fuel* **2006**, *20* (2), 668-672.

(22) McKenna, A. M.; Marshall, A. G.; Rodgers, R. P. Heavy petroleum composition. 4. Asphaltene compositional space. *Energy Fuel* **2013**, *27* (3), 1257-1267.

(23) Tong, J.; Liu, J.; Han, X; Wang, S.; Jiang, X. Characterization of nitrogen-containing species in Huadian shale oil by electrospray ionization Fourier transform ion cyclotron resonance mass spectrometry. *Fuel* **2013**, *104*, 365-371.

(24) Bae, E.; Na, J. G.; Chung, S. H.; Kim, H. S.; Kim, S. Identification of about 30 000 Chemical Conponents in shale Oils by Electrospray ionization (ESI) and Atmospheric Pressure Photoionization (APPI) Coupled with 15 T Fourier Transform Ion Cyclotron

Resonance Mass Spectrometry (FT-ICR MS) and a Comparison to Conventional Oil. *Energy Fuel* **2010**, *24* (4), 2563-2569.

(25) Chen, X.; Shen, B.; Sun, J.; Wang, C.; Shan, H.; Yang, C.; Li, C. Characterization and comparison of nitrogen compounds in hydrotreated and untreated shale oil by electrospray ionization (ESI) Fourier Transform ion cyclotron resonance mass spectrometry (FT-ICR MS). *Energy Fuel* **2012**, *26* (3), 1707-1714.

(26) Jin, J.M.; Kim, S.; Birdwell, J.E. Molecular characterization and comparison of shale oils generated by different pyrolysis methods. *Energy Fuel* **2012**, *26*, 1054-1062.

(27) Littke, R.; Baker, D. R.; Leythaeuser, D. Microscopic and sedimentologic evidence for the generation and migration of hydrocarbons in Toarcian source rocks of different maturities. *Org Geochem* **1988**, *13* (1–3), 549-559.

(28) Rullkötter, J.; Marzi, R. Natural and artificial maturation of biological markers in a Toarcian shale from northern Germany. *Org Geochem* **1988**, *13* (4–6), 639-645.

(29) Mann, U.; Müller, P. J. Source rock evaluation by well log analysis (Lower Toarcian, Hils syncline). *Org Geochem* **1988**, *13* (1–3), 109-119.

(30) Littke, R.; Leythaeuser, D.; Rullkötter, J.; Baker, D. R. Keys to the depositional history of the Posidonia Shale (Toarcian) in the Hils Syncline, northern Germany. *Geological Society, London, Special Publications* **1991**, *58* (1), 311-333.

(31) Rullkötter, J.; Leythaeuser, D.; Horsfield, B.; Littke, R.; Mann, U.; Müller, P. J.; Radke, M.; Schaefer, R. G.; Schenk, H. J.; Schwochau, K.; Witte, E. G.; Welte, D. H. Organic matter maturation under the influence of a deep intrusive heat source: A natural experiment for quantitation of hydrocarbon generation and expulsion from a petroleum source rock (Toarcian shale, northern Germany). *Org Geochem* **1988**, *13* (4–6), 847-856.

(32) Schulz, H.-M.; Horsfield, B.; Sachsenhofer, R. F. Shale gas in Europe: a regional overview and current research activities. *Geological Society, London, Petroleum Geology Conference series* **2010**, *7*, 1079-1085.

(33) Shipkova, P. A.; Heimark, L.; Bartner, P. L.; Chen, G. D.; Pramanik, B. N.; Ganguly, A. K.; Cody, R. B.; Kusai, A. High-resolution LC/MS for analysis of minor components in complex mixtures: negative ion ESI for identification of impurities and degradation products of a novel oligosaccharide antibiotic. *J Mass Spectrom* **2000**, *35* (11), 1252-1258.

(34) Quirk, M.M.; Wardroper, A.M.K.; Wheatley, R.E.; Maxwell, J.R. Extended hopanoids in peat environments. *Chem Geol* **1984**, *42*, 25-43.

(35) Watson, D.F. and Farrimond, P. Novel polyfunctionalised geohopanoids in a recent lacustrine sediment (Priest Pot, UK). *Org Geochem* **2000**, *31*, 1247-1252.

(36) Farrimond, P.; Griffiths, T.; Evdokiadis, E. Hopanoic acids in Mesozoic sedimentary rocks: their origin and relationship with hopanes. *Org Geochem* **2002**, *33*, 965-977.

(37) Bennett, B. and Abbott, G.D. A natural pyrolysis experiment – hopanes from hopanoic acids? *Org Geochem* **1999**, *30*, 1509-1516.

(38) Horsfield, B. and Düppenbecker, S.J. The decomposition of Posidonia Shale and Green River Shale kerogens using Microscale Sealed Vessel (MSSV) pyrolysis. *J Anal Appl Pyrol* **1991**, *20*, 107-123.

(39) Szabo, A.; Suhr, H.; Venugopalan, M. Decarbonylierung von Chinonen. *Liebigs Annalen der Chemie* **1977**, *5*, 747-759.

Corresponding Author

*Tel +49-331-288-1796. E-mail address: poetz@gfz-potsdam.de

Notes

The authors declare no competing financial interest.

ACKNOWLEDGMENT

The authors wish to thank C. Karger for sample preparation and technical assistance.

Supporting Information

Maturity-driven Generation and Transformation of Acidic Compounds in the Organic-rich Posidonia Shale as revealed by Electrospray Ionization Fourier Transform Ion Cyclotron Resonance Mass Spectrometry

Stefanie Poetz[*]*, Brian Horsfield and Heinz Wilkes*

GFZ German Research Centre for Geosciences, Telegrafenberg, D-14473 Potsdam

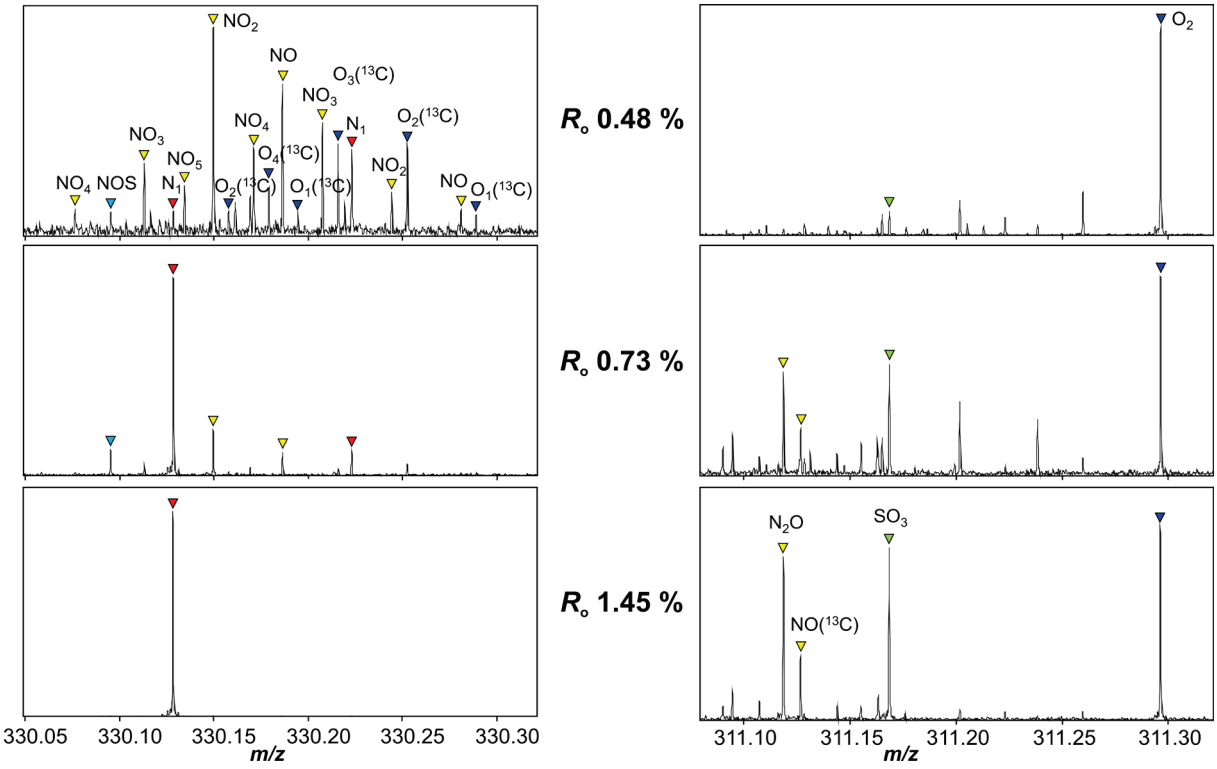

Figure SI 1: A more detailed view into the enlarged mass segments of two nominal masses m/z 330 (contains the most abundant peak in the most mature sample HAD) and m/z 311 (contains the most abundant peak in the least mature sample WE) of the WE, DO and HAD samples. The spectrum of the immature WE sample contains a number of peaks with an even nominal mass m/z 330 in low abundance representing a variety of compound types, e.g. different N1Ox compounds with 1 to 5 oxygen atoms. Almost all these compounds decrease with increasing maturity (DO sample) until there is only the signal of the N1 compounds left

at Ro 1.45 % (sample HAD). For the odd nominal mass m/z 311, the opposite is observed: for low maturities, there is only one signal of an O2 compound in the spectrum, while at Ro 1.45 %, additional signals of other compounds like N2O1 or S1O3 arise.

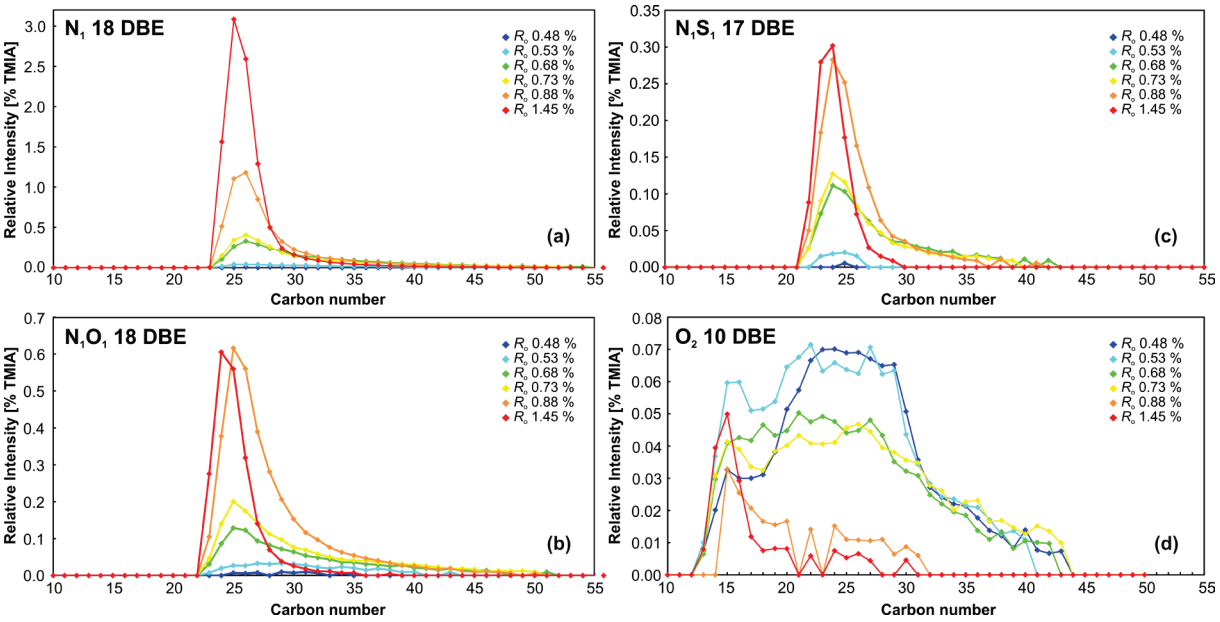

Figure SI 2: Carbon number distributions of the N_1 18 DBE class (a), N_1O_1 18 DBE class (b), N_1S_1 17 DBE class (c) and O_2 10 DBE class (d) of the six Posidonia Shale samples.

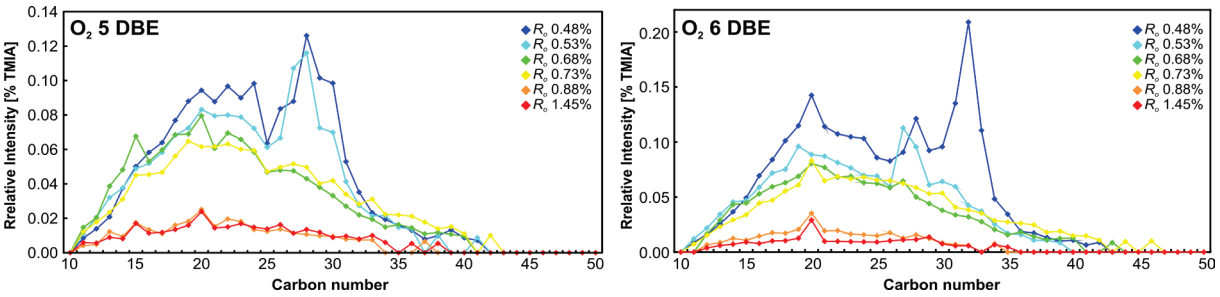

Figure SI 3: Carbon number distributions of the O_2 5 DBE class containing the steroidal acids ($C_{27\text{-}29}$) and of the O_2 6 DBE class containing the hopanoid acids ($C_{28\text{-}36}$) which both are enriched in the immature samples.

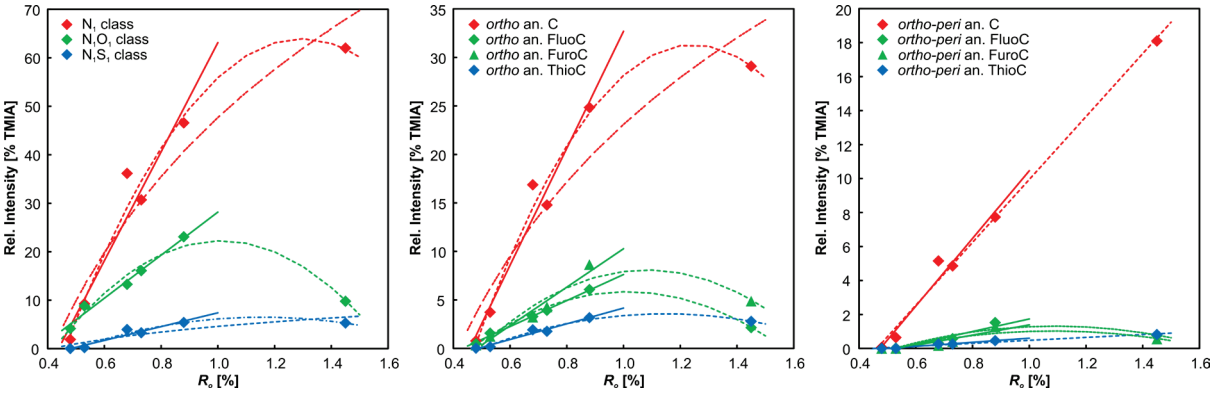

Figure SI 4: Maturity-related changes in relative abundances of a) the N_1, N_1O_1 and N_1S_1 compound classes, b) the *ortho*-fused carbazoles, fluorenonocarbazoles, furanocarbazoles and thiophenocarbazoles and c) the *ortho*- and *peri*-fused carbazoles, fluorenonocarbazoles, furanocarbazoles and thiophenocarbazoles.

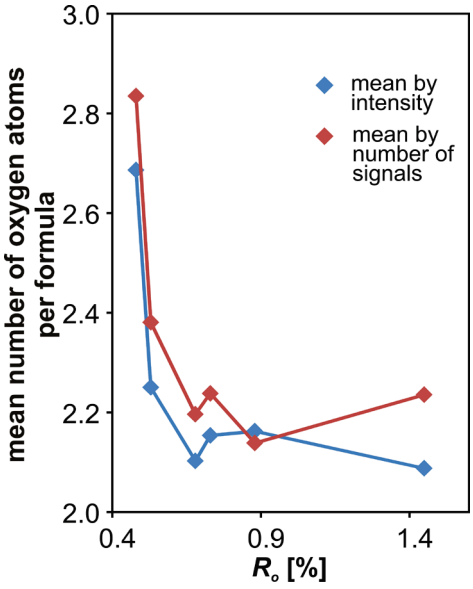

Figure SI 5: The mean number of oxygen atoms (mean by intensity and mean by number of signals) decreases with increasing maturity.